A case study of non-displacement piles in pliocene sands

Une étude de cas sur des pieux sans déplacement dans sables du Pliocène

Jaime A. Santos
Instituto Superior Técnico, Technical University of Lisbon, Portugal

M. Matos Fernandes
Faculty of Engineering, University of Porto, Portugal

Mário P. Costa, André Correia & Pedro Oliveira
Fase, Estudos e Projectos, Porto, Portugal

ABSTRACT

The paper focuses on the foundation piles of a very large industrial plant located in the peninsula of Setúbal, Portugal. The ground is composed by a thick deposit of Pliocene sands and silty sands, with the water table close to the surface. Bored piles drilled under bentonite slurry of diameters from 0.5 m to 1.0 m were adopted with lengths up to 22 m. The site was carefully characterized. A number of static and dynamic axial load tests on prototype piles were carried out, providing the evaluation of the base and the shaft resistance. The results of these tests are discussed and compared with the ones obtained from a semi-empirical method based on in situ ground tests.

RÉSUMÉ

Le papier focalise les pieux de fondation d'une usine industrielle de grande dimension située dans la péninsule de Setúbal, Portugal. Le terrain se compose par un dépôt épais de sables limoneux du Pliocène, avec la nappe phréatique près de la surface. Des pieux forés à la boue de diamètres de 0.5 m à 1.0 m ont été adoptés avec des longueurs jusqu'à 22 m. L'emplacement a été soigneusement caractérisé. Un certain nombre d'essais axiaux statiques et dynamiques de chargement sur des pieux de prototype ont été effectués, fournissant l'évaluation de la résistance de pointe et de frottement latéral. Les résultats de ces essais sont discutés et comparés à ceux obtenus à partir d'une méthode semi-empirique basée sur les essais au sol in situ.

Keywords: Pile, static load test, dynamic load test, installation effects

1 INTRODUCTION

Design methods, observation of pile performance during installation and loading, and soil-pile interaction analysis are key aspects for a complete understanding of pile behaviour.

Despite recent advances on the comprehension of the changes that occur in the soil around axially loaded piles, common design calculations heavily rely on empirical correlations (D'Aguiar, 2008). The use of the CPT cone resistance provides a good basis for these calculations but care must be taken in data extrapolation from empirical correlations or even from pile load tests (static or dynamic) to pile geometries and soil conditions outside the current database, in order to ensure the correct consistency with the actual conditions.

The weak reliability of the prediction methods (Viana da Fonseca and Santos, 2008) and the clear influence of installation techniques on the performance are closely related. In fact, the limitations in characterizing the installation method prevent the improvement of prediction methods and, in addition, disable the optimization of some of the installation techniques. Therefore load tests on instrumented piles can play a major role to check bearing capacity and settlement calculations.

2 SITE DESCRIPTION

The paper describes the design and the static and dynamic tests of bored piles used for founding large industrial buildings. The site is located in Setúbal, 50 km to the south of Lisbon, between the valleys of the Tagus and Sado rivers, not far from the Atlantic coast. In the geological chart of Portugal the site corresponds to Pliocene formations, consisting of sands, silty sands, clayey sands, with thin lenses of sandy and silty clays.

The field geotechnical characterization consisted of: i) 91 conventional boreholes with SPTs and (disturbed) sampling; ii) 4 groups of cross-hole seismic tests, close to 4 boreholes; iii) 12 CPTs. In general, the depth reached by the CPT was small, ranging from 1.6 m to 9.4 m (average 5 m). Grain size distribution and Atterberg limits were evaluated in the lab together with some triaxial compression tests on reconstituted samples.

The interpretation of the results provided by that characterization permitted the division of the ground in four Geotechnical Horizons, from GH4 (the shallowest) to GH1 (the deepest), as shown in Table 1.

Table 1. Geotechnical Horizons of the ground (from the surface).

Horizon	Description	$N_{SPT} = N_{60}$
GH4	Organic soils, man-made fill	≤ 10
GH3	Sands, silty and clayey sands, interspersed with thin layers and lenses of sandy and silty clays (Pliocene)	11 - 29
GH2	Sands, silty and clayey sands and, sparsely, sandy or silty clays (Pliocene)	30 - 60
GH1	Sands, silty and clayey sands and, sparsely, sandy clays (Pliocene)	> 60

The thickness of GH4 is generally small. GH1 forms the substratum and is normally found at 12-15 m depth. Between these two extreme horizons, the disposition of the other is rather complex: GH2 may occur on GH3 and, even, GH1 (then called GH1A) may be found on or in between GH2 and GH3.

Figure 1 presents results of field tests at one of the locations where pile load tests have been carried out.

Proceedings of the 17th International Conference on Soil Mechanics and Geotechnical Engineering
M. Hamza et al. (Eds.)

doi:10.3233/978-1-60750-031-5-1232

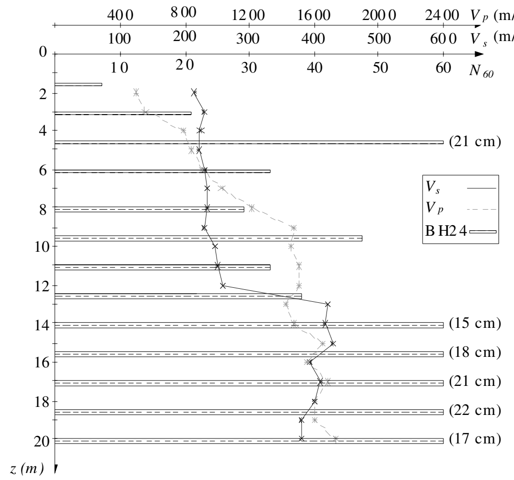

Figure 1. SPT and cross-hole results at the location of borehole BH24.

3 COMPRESSIVE RESISTANCE FROM GROUND TEST RESULTS

In view of the variability of the geotechnical characteristics, both in depth and in plan, the site was divided in distinct Design Zones, corresponding to boreholes whose results could be considered reasonably alike. The intention was to achieve a common solution for each zone concerning the pile foundations.

The evaluation of the bearing capacity of the piles was done on the basis of the method developed by Bustamante and Gianeselli (1983).

Since the CPT did not reach the relevant horizons controlling the pile behaviour, for applying the method mentioned above the values of q_c have been evaluated through N_{SPT}, applying the correlation proposed by Robertson and Campanella (1983).

The adopted procedure involved the following steps:

a) Definition of the Design Zones taking into account, particularly, the depth of the substratum, the distribution of the Geotechnical Horizons defined in Table 1 and the proximity of the boreholes.

b) For the boreholes of each Design Zone and for each Geotechnical Horizon, calculation of the mean value of D_{50}.

c) For the boreholes of each Design Zone and for each Geotechnical Horizon, calculation of the mean value of the ratio q_c/N_{SPT} from the chart of Robertson and Campanella (1983).

d) For each borehole, calculation of q_c values, on the basis of the values of N_{SPT}; these, when corresponding to tests with refusal ($N_{SPT} > 60$), were corrected taking into account the actual penetration length.

e) For the boreholes of each Design Zone, and for each Geotechnical Horizon, computation of the characteristic values of q_c corresponding to the fractile of 5%, assuming a normal distribution, q_{ck}.

f) For the boreholes of each Design Zone and for each Geotechnical Horizon, selection of the characteristic values of the shaft resistance, q_{sk}, on the basis of q_{ck} and of the values of a and q_{smax} as defined by Bustamante and Gianeselli.

g) For the boreholes of each Design Zone and for the Geotechnical Horizon 1, selection of the characteristic value of the base resistance, q_{bk}, on the basis of q_{ck} and taking the coefficient k_c (Bustamante and Gianeselli, 1983), equal to 0.3.

h) For each Design Zone and for each pile diameter (diameters from 500 to 1000 mm), iterative fitting of the pile length in order to obtain design compressive resistance values, R_d, greater than or equal to the vertical loads calculated in the design of the structure (corresponding to a maximum compressive stress in the pile of 5 MPa, in SLS conditions); a minimum penetration of 3 diameters in the substratum was imposed; partial safety factors of 2.0 and 3.0 were taken for the shaft and the base resistance, respectively.

i) Iterative fitting of the distribution of the boreholes among the distinct Design Zones, in order to minimize the variance of R_d; repetition of the steps a) to h) until stabilizing the solution.

This procedure led to the definition of five Design Zones, and to pile length values ranging from 16 m to 22 m. Table 2 presents, for Design Zones 1, 2 and 4, the mean and the characteristic values of q_c, q_b and q_s as well as the standard deviation associated to the distribution of q_c.

Table 2. Mean and characteristic values of q_c, q_s and q_b for Design Zones 1, 2 and 4.

		Geotechnical Horizon			
		1	1A	2	3
Design Zone 1	q_{cm} [MPa]	68.3	51.8	23.4	13.8
	σ_{qc}	29.3	9.1	4.5	3.3
	q_{ck} [MPa]	20.1	36.8	16.0	8.3
	q_{bm} [MPa]	20.5	-	-	-
	q_{bk} [MPa]	6.0	-	-	-
	q_{sm} [kPa]	120.0	120.0	80.0	70.7
	q_{sk} [kPa]	120.0	120.0	80.0	46.1
Design Zone 2	q_{cm} [MPa]	70.4	47.9	26.6	10.3
	σ_{qc}	27.7	10.3	9.1	3.4
	q_{ck} [MPa]	25.0	31.0	11.7	4.7
	q_{bm} [MPa]	21.1	-	-	-
	q_{bk} [MPa]	7.5	-	-	-
	q_{sm} [kPa]	120.0	120.0	80.0	55.9
	q_{sk} [kPa]	120.0	120.0	65.2	25.9
Design Zone 4	q_{cm} [MPa]	55.8	53.9	24.4	11.8
	σ_{qc}	15.8	14.0	5.1	2.8
	q_{ck} [MPa]	29.8	30.8	16.1	7.3
	q_{bm} [MPa]	16.7	-	-	-
	q_{bk} [MPa]	8.9	-	-	-
	q_{sm} [kPa]	120.0	120.0	80.0	65.2
	q_{sk} [kPa]	120.0	120.0	80.0	40.6

The application of the design procedure described above to the borehole closer to the pile load tests ES1 and EI1 (borehole BH24, Figure 1) and the pile load test EI2 (boreholes BH57 and BH58), led to the results summarized in Table 3. The actual pile lengths (about 16 m) and pile diameter (800 mm) were considered for a proper comparison. As indicated in the tables, borehole BH24 was included in the Design Zone 1, borehole BH57 was included in the Design Zone 4 and borehole BH58 belongs to Design Zone 2.

Table 3 – Summary of the computation of the compressive resistance of piles ES1, EI1 and EI2 on the basis of ground test results.

Pile load tests ES1 and EI1				Pile load test EI2							
BH24 (Design Zone 1)				BH57 (Design Zone 4)				BH58 (Design Zone 2)			
Geot. Hor.	L_i [m]	q_{ski} [kPa]	q_{smi} [kPa]	Geot. Hor.	L_i [m]	q_{ski} [kPa]	q_{smi} [kPa]	Geot. Hor.	L_i [m]	q_{ski} [kPa]	q_{smi} [kPa]
3	1.16	46	71	3	6.65	41	65	2	0.24	65	80
1A	1.50	120	120	1A	3.00	120	120	3	1.50	26	56
2	2.00	80	80	2	1.50	80	80	2	3.50	65	80
3	1.50	46	71	1	3.55	120	120	1	9.46	120	120
2	4.50	80	80								
1	3.54	120	120								
Characteristic values			Mean values	Characteristic values			Mean values	Characteristic values			Mean values
R_{sk}	3135	kN	R_{sm} 3300 kN	R_{sk}	2955	kN	R_{sm} 3367 kN	R_{sk}	3563	kN	R_{sm} 3816 kN
R_{bk}	3030	kN	R_{bm} 10304 kN	R_{bk}	4495	kN	R_{bm} 8394 kN	R_{bk}	3763	kN	R_{bm} 10606 kN
R_d [SLS]	2578	kN	R_m 13604 kN	R_d [SLS]	2976	kN	R_m 11761 kN	R_d [SLS]	3036	kN	R_m 14422 kN
R_d [ULS]	3927	kN		R_d [ULS]	4521	kN		R_d [ULS]	4622	kN	

4 LOAD TESTS

A load test program was prepared with the aim of determining the response of representative piles both in terms of settlement and limit load. The program consisted of 5 static load tests and 3 dynamic impact load tests. In the static load tests 3 of them had only measurements of the load and the settlement at the pile head (bored piles ES4, ES5 and ES2) while in the other 2 tests the piles were fully instrumented with strain gauges in such a manner that the base and shaft resistance can be derived separately from the measurements (bored piles EI1 and EI2).

Figures 2 and 3 refer to piles EI1 and EI2, respectively, with the soil profile and the load distribution corresponding to a load stage close to the expected SLS load and to the maximum test load. Some gauge levels were eliminated from the analysis due to measurement imprecision (error).

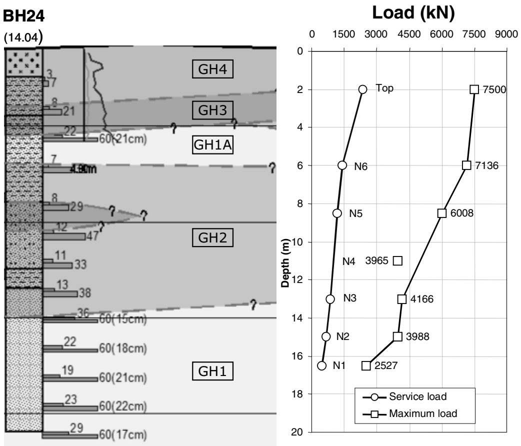

Figure 2. Static load test on pile EI1.

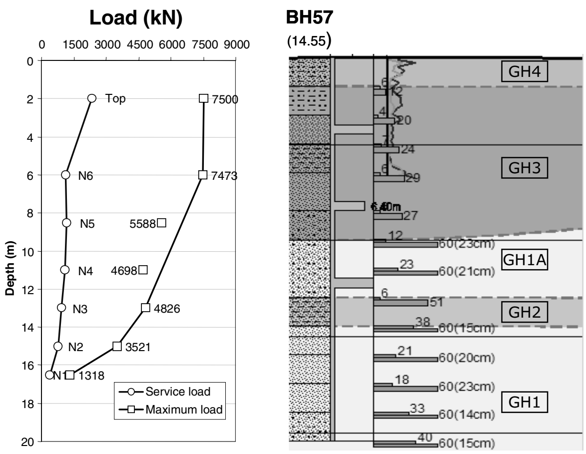

Figure 3. Static load test on pile EI2.

The dynamic load tests on piles ES1 (bored pile), RS1 and RS2 (CFA piles) were performed using a 19 ton free-fall hammer. The test procedure followed two different stages. Initially, a set of blows with increasing falling height was applied (0.3 to 2 m). Afterwards the energy was kept constant for the maximum falling height (2 m). With this test procedure it was possible to study the evolution of the total resistance (impacts with increasing falling height) and the evolution of the shaft resistance (several impacts with constant falling height). The instrumentation consisted of 4 strain transducers and 4 accelerometers attached to the pile head. Signal matching techniques were used to derive the shaft resistance and the base resistance and to simulate the static load-settlement curve. Figure 4 refers to pile ES1 with the soil profile and the distribution of the unit shaft resistance obtained from the dynamic load test.

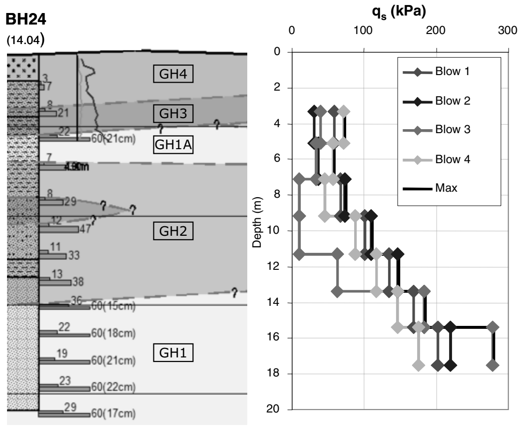

Figure 4. Dynamic load test on pile ES1.

The parabolic shape of the load distribution curve (Figures 2 and 3) and the almost linear distribution of the unit shaft resistance (Figure 4) are in agreement with the soil conditions and with the increase of effective stresses with depth.

5 DISCUSSION OF RESULTS

The following figures show the load-settlement curves of the piles allowing a direct comparison of the results. Figure 5 refers only to the static tests, while Figure 6 provides a comparison of load-settlement curves of static and dynamic load tests.

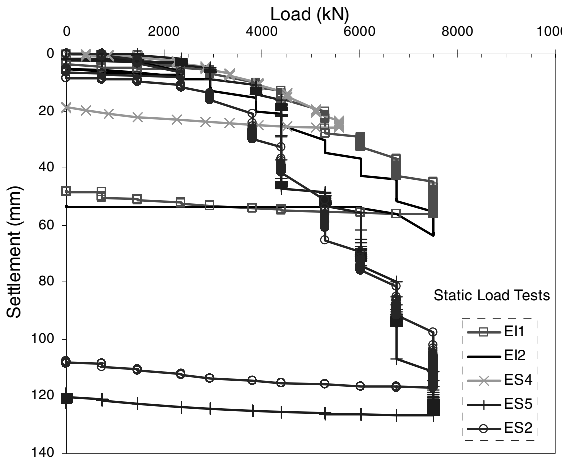

Figure 5. Load-settlement curves from static load tests.

From the analysis of Figures 5 and 6 one can observe quite a distinct response in the various piles. The piles EI1, EI2 and ES4 (the latter has a diameter of 600 mm) had better performance highlighting the progressive mobilization of the shaft resistance and the base resistance. On the contrary, piles ES2 and ES5 exhibited quite high settlements, mainly for load stages beyond 3000 kN.

Although some differences in soil conditions occur among the locations of the distinct load tests, the discrepancies in the pile load test results are probably due to installation effects, which have a strong influence on the mobilization of the shaft and mostly of the base resistance of non-displacement piles.

The comparison of load-settlement curves shown in Figure 6 reveals a satisfactory agreement between the dynamic and the static load tests for loads up to 3000 kN. For higher loads, the accordance is only good between piles EI1 and EI2 (static load tests) and ES1, RS1 and RS2 (dynamic load tests).

Figure 7 shows the distribution of the unit shaft resistance (q_s) determined from the dynamic load tests. For the static load tests the unit shaft resistance can be calculated from the change of load between the strain-gauge levels divided by their distance and pile perimeter. However, such differentiation can originate erratic distributions of q_s due to imprecision of the strain measurements and their conversion to load in the piles. Therefore, only average values of the unit shaft resistance were calculated for the upper horizons (GH2 and GH3) and for the lower horizon (GH1) (see Table 4).

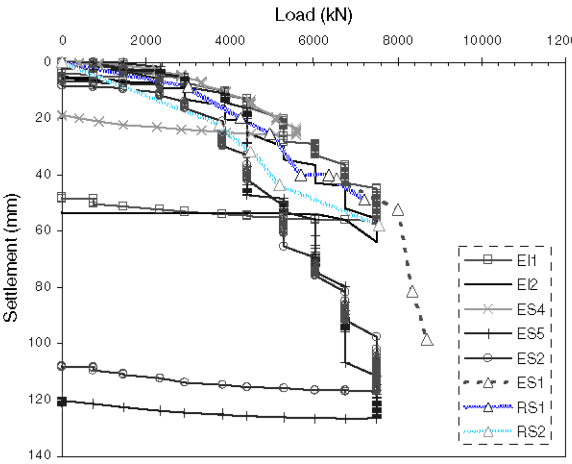

Figure 6. Load-settlement curves from static and dynamic load tests.

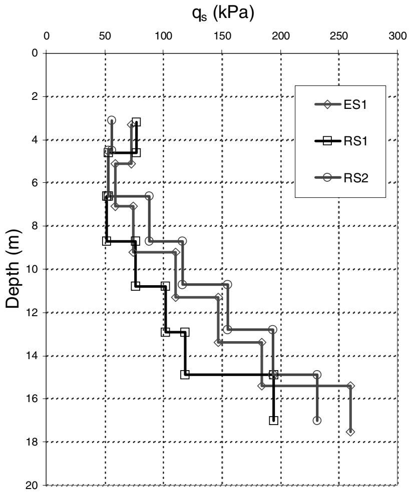

Figure 7. Unit shaft resistance from dynamic load tests.

Table 4 presents a summary of the compressive axial pile resistance and the unit shaft resistance obtained from the load tests. To determine the compressive pile resistance, a settlement of the pile head equal to 10% of the pile diameter was adopted as failure criterion.

Table 4. Summary of pile load tests results.

Load Test		Static	Static	Dynamic
Pile		EI1	EI2	ES1
Diameter	(mm)	800	800	800
Q_{ser} / s	(kN)/(mm)	2400 / 5.4	2400 / 7.2	2400 / –
Q_{max} / s_{max}	(kN)/(mm)	7500 / 56.1	7500 / 63.7	8700 / –
$R_{10\%}$	(kN)	> 7500	> 7500	≈ 8700
$R_{b10\%}$	(kN)	> 2530	>1320	> 4776
$R_{s10\%}$	(kN)	< 4970	< 6180	> 3924
$q_{s,(GH2\ \&\ GH3)}$	(kPa)	100	120	105 (60 – 150)
$q_{s,(GH1)}$	(kPa)	> 180	> 120 - 140	180 - 280

Q_{serv} – load stage close to the expected SLS load ; s – settlement at Q_{serv}
Q_{max} – maximum test load ; s_{max} – settlement at maximum test load
$R_{10\%}$ – total resistance ; $R_{b10\%}$ – base resistance ; $R_{s10\%}$ – shaft resistance
$q_{s,\ (GH2\ \&\ GH3)}$ – average unit shaft resistance for GH2 and GH3
$q_{s,\ (GH1)}$ – average unit shaft resistance for GH1

One can see from Figure 6 and Table 4 that the ultimate resistance lies in the range between 6100 kN and 8700 kN, which is much lower than the mean values indicated in Table 3 (11761 kN to 14422 kN), mainly due to overestimation of the base resistance by the semi-empirical method.

Regarding the unit shaft resistance, the values obtained from the static load tests are in good agreement with the average values derived from the dynamic load tests. The values vary between 100 kPa and 120 kPa for the upper horizons (GH2 and GH3) and between 150 kPa and 180 kPa for the lower horizon (GH1). Therefore the shaft resistance is underestimated by the semi-empirical method (see values of q_{sm} in Table 2).

6 CONCLUSIONS

The paper presents a case on non-displacement piles in Pliocene sands, with the compressive axial resistance of the piles being evaluated by a semi-empirical method using in situ soil tests and by static and dynamic load tests. The overall analysis of the results allowed the following conclusions to be drawn.

The combined execution of static and dynamic load tests permitted the assessment of the compressive resistance, with comparable results and similar load-settlement curves.

For the expected service load, the settlements were generally less than 8 mm with the predominant contribution of the shaft resistance. For the maximum load, the settlements were, in some cases, quite high and there was an important mobilization of the base resistance.

The mean values of the compressive pile resistance estimated by the semi-empirical method correspond to an overestimation of the resistance found in the load tests. The main reason may be attributed to the high values of q_c obtained from correlation with N_{SPT} in refusal conditions ($N_{SPT} > 60$).

In two test piles the response was clearly different from the other ones and the reason cannot be simply assigned to soil variability; this is a clear indication of the installation effects, which have a strong influence on the mobilization of the shaft and, mostly, of the base resistance of non-displacement piles.

The application of Eurocode 7 to the results of the pile load tests would provide values of the design compressive resistance for ULS in reasonable agreement with those presented in Table 3, calculated through the semi-empirical method. Then, the safety conditions would be satisfied by both methodologies.

The resistances found in the pile load tests are satisfactory for the pile design loads, both for SLS and ULS conditions. Moreover, the working piles had a minimum length of 18 m, about 2 m more than the test piles, which means that the design was sufficiently conservative.

ACKNOWLEDGEMENT

The authors wish to express their thanks to PORTUCEL SOPORCEL GROUP for permitting the presentation of the results of pile design and testing.

REFERENCES

Bustamante M. and Gianeselli L. 1983. Calcul de la capacité portante des pieux à partir des essais au pénétromètre statique. *Bulletin de Liaison des Lab. des Ponts et Chaussées*, 127, pp. 73–80.

D'Aguiar, S. 2008. Numerical Modelling of Soil-Pile Load Transfer Mechanisms in Granular Soils. *PhD dissertation. École Centrale Paris*, pp. 339.

Robertson, P. K. and Campanella, R. G. 1983. Interpretation of cone penetrometer test: Part I: Sand. *Canadian Geotechnical Journal*, 20(4), pp. 718-733.

Viana da Fonseca, A. and Santos, J.A. 2008. International Prediction Event. Behaviour of Bored, CFA and Driven Piles in Residual Soil. ISC'2 Experimental Site, *Pub. Univ. of Porto (FEUP) & Tech. Univ. of Lisbon (IST-UTL)*, pp. 699.